Combining Robust Expectation Maximization and Mean Shift algorithms for Multiple Sclerosis Brain Segmentation

Daniel García-Lorenzo, Sylvain Prima, D. Louis Collins, Douglas Arnold, Sean Patrick Morrissey, Christian Barillot

Combining Robust Expectation Maximization and Mean Shift algorithms for Multiple Sclerosis Brain Segmentation

Daniel García-Lorenzo[1,2,3] ⋆, Sylvain Prima[1,2,3], D. Louis Collins[4], Douglas L. Arnold[4], and Sean P. Morrissey[1,2,3,5] Christian Barillot[1,2,3]

[1] INRIA, VisAGeS Unit/Project, IRISA, Rennes, France
[2] University of Rennes I, CNRS IRISA, Rennes, France
[3] INSERM, U746 Unit/Project, IRISA, Rennes, France
[4] Montreal Neurological Institute and Hospital, McConnel Brain Imaging Centre, Montreal, Canada
[5] Department of Neurology, University Hospital Pontchaillou, Rennes, France

Abstract. A new algorithm for segmentation of white matter lesions and normal appearing brain tissues in Multiple Sclerosis (MS) is presented. Two different segmentation methods are combined in order to have a better and more meaningful segmentation. On the one hand, a local segmentation approach, the Mean Shift, is used to generate local regions in our images. On the other hand, a variant of the Expectation Maximization is employed to classify these regions as Normal Appearing Brain Tissues (NABT) or lesions. Validation of this method is performed with synthetic and real data. The output is a more powerful algorithm that employs at the same time global and local information to improve image segmentation.

1 Introduction

Multiple Sclerosis (MS) is a chronic disease of the central nervous system leading eventually to severe handicap. Magnetic Resonance Imaging (MRI) serves as a sensitive biomarker for diagnostic, prognosis and follow up, especially in clinical trials [1]. The automatic segmentation of MS white matter lesions (WML) and NABT in MRI is a challenging task for image processing.

Most segmentation algorithms can be roughly divided into either global or local depending on the information they use. Global methods try to extract information from the whole image and then use this information to classify each voxel independently [2, 3]. This is the case of all clustering- or histogram-based segmentation methods. In some cases some spatial information is introduced into these methods by using Markov Random Fields [4] or probabilistic atlas [5].

On the other hand, local methods use exclusively local information to create, in many cases, an undetermined number of local regions. The challenge of these

⋆ We are thankful to ARSEP for funding

methods is to combine these local regions to build a global and meaningful segmentation [6]. One such local method is the Mean Shift (MeS[6]) [7]. MeS is an unsupervised and non-parametric gradient density estimation algorithm that has been successfully applied in clustering, segmentation and filtering of natural 2D images [8]. Recently, it has been applied, in two different ways, in the segmentation of brain MRI of healthy volunteers [9, 10]. The first method uses an atlas to label the regions given by the MeS in three classes (white matter (WM), grey matter (GM) and cerebrospinal fluid (CSF)). The second method performs an Expectation Maximization (EM) algorithm [11] over the image intensities in order to estimate a 3-class Finite Gaussian Mixture Model (FGMM), and then assigns each MeS region to the class with highest probability.

To our knowledge, none of those local methods has been applied to WML and NABT segmentation in MS patients. However, local information potentially should improve the contour delineation of the WML and NABT as it only uses local information. Global information is needed then to reduce the number of MeS regions for the final segmentation. Here, we propose to improve Mayer's approach[10] by replacing the original EM by a robust EM (mEM) algorithm [12], that was successfully applied in MS patients[2].

The paper is structured as follows: in Section 2.1, we briefly describe the MeS approach, then in Section 2.2 the mEM is presented. Section 2.3 describes the complete segmentation algorithm. In Section 3 the algorithm is tested with synthetic and real images. Section 4 presents the conclusions of this work.

2 Methods

2.1 The Mean Shift algorithm

Theory The Mean Shift algorithm is a non-parametric technique for the probability density gradient estimation [7] with multiple applications [8], one of them being the image segmentation.

Given n data points x_i, $i = 1, .., n$ in the d-dimensional space R^d the Parzen window density estimator, with spherical kernel $K(x)$ (whose profile kernel is named $k(x)$) and one bandwidth parameter b, is given by

$$\hat{f}_{b,k}(x) = \frac{1}{nb^d} \sum_{i=1}^{n} k\left(\left\| \frac{x - x_i}{b} \right\|^2 \right) \tag{1}$$

The gradient of the density can be estimated as

$$\hat{\nabla} f(x) \equiv \nabla \hat{f}_{b,k} = \frac{2}{nb^{d+2}} \sum_{i=1}^{n} (x - x_i)\, k'\left(\left\| \frac{x - x_i}{b} \right\|^2 \right) \tag{2}$$

Then if we define $g(x) = -k'(x)$ we call the "mean shift vector" the difference between the weighted mean and the center of the kernel.

[6] Mean Shift abbreviation is normally MS but in this article MS is reserved for Multiple Sclerosis

$$m_{b,g}(x) = \frac{\sum_{i=1}^{n} x_i g\left(\left|\left|\frac{x-x_i}{b}\right|\right|^2\right)}{\sum_{i=1}^{n} g\left(\left|\left|\frac{x-x_i}{b}\right|\right|^2\right)} - x \tag{3}$$

The mean shift vector always points towards the direction of maximum increase of the density [8]. For each point x, the mean shift vector $m_{b,G}(x)$ is calculated and then the center of the kernel is translated by $m_{b,G}(x)$. Convergence is guaranteed to a zone of zero gradient and local maximum of density, called mode. All the points that converge to the same mode M, are given the same label and form a region.

MeS for 3D images The MeS algorithm can be used in two different ways for image segmentation. The first option is to use it as a clustering technique where a point x_i has the dimension $d = m$, where m is the number of different MR sequences. In that case, the MeS is performed on the joint intensity histogram. Another approach is to add the three spatial dimensions to the feature vector having $d = 3 + m$ so that the classification will be done in the joint spatial-intensity domain [8]. This last option is more adapted because it also integrates the spatial information in the classification. As spatial information and intensity information have different nature, the kernel $K(x)$ can be decomposed into two kernels allowing two different bandwidth parameters, one for spatial components b_s and another one for intensity components b_r, as:

$$K_{b_s,b_r}(x) = K\left(\frac{x^s}{b_s}\right) K\left(\frac{x^r}{b_r}\right) \tag{4}$$

where x^s contains the three spatial dimensions and x^r the m intensity components. Segmentation methods using the same parameter b for both kernels [10] can be inefficient because of an improper normalization between spatial and intensity dimensions.

2.2 The modified EM

A 3-class FGMM [4, 5] is used to model NABT intensities. All the MR sequences are used to create a multidimensional feature space in order to benefit from the specific inherent information of each sequence. The EM algorithm has been widely used for estimating the NABT parameters in healthy volunteers and in MS patients [4, 5]. Recently a robust modified EM (mEM) has been used for automatic WML segmentation [2]. This method performs a good estimation of NABT parameter although it does not have any spatial constraints to improve the segmentation results.

The mEM allows to compute the trimmed likelihood estimator [12] and has a monotonous convergence, at least to a local maximum of the trimmed likelihood (TL), as the original EM algorithm. The idea is to use exclusively in our computation of trimmed likelihood the $n - h$ voxels that are close to the model

and reject the h voxels more likely to be outliers.

$$TL = \sum_{i=1}^{n-h} f(x_{\nu(i)}; \Theta) \tag{5}$$

where n is the total number of voxels, h the number of rejected voxels, x_i is a vector with the intensities of the m sequences of the voxel i, Θ the parameters of our 3-class model, $f()$ the probability density function of the model and $\nu()$ is a permutation function which sorts voxels so that:

$$f(x_{\nu(1)}; \Theta) \geq f(x_{\nu(2)}; \Theta) \geq ... \geq f(x_{\nu(n)}; \Theta) \tag{6}$$

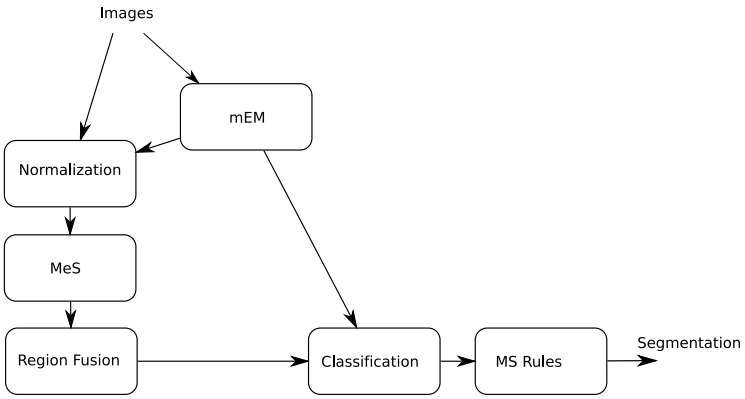

Fig. 1. Workflow of REMMeS algorithm. Each step is described in Section 2.3

2.3 REMMeS: Robust Expectation Maximization with Mean Shift

Figure 1 displays the workflow of this method with all the steps explained in the following.

NABT Model estimation (mEM) The image intensities in a healthy brain are usually modelled as a 3-class FGMM [2]. In the case of MS patients, the WML can bias the estimation of the model if we use a classical EM algorithm. In our case, we use the mEM explained in Section 2.2 with $h = \frac{n}{10}$. This value is large enough to ensure that all the lesions are not used in the estimation of the parameters of our model.

Sequence Normalization (Normalization) Different MR sequences have different tissue variances so the bandwidth parameter b_r may be inefficient. In (4), the kernel can be decomposed to have one b_r parameter per sequence but

this increases the processing time of the algorithm. Our solution is to normalize the image intensity of each sequence so that the WM variance is 1.0, using the WM parameters estimated by the mEM algorithm.

MeS segmentation (MeS) MeS algorithm creates an undetermined number of output regions using only local information. Two parameters have to be tuned: b_s and b_r. Small values create an oversegmentation and make MeS more sensitive to noise while large values tend to eliminate small regions, such as the WML. After several tests in real and synthetic images, those values have been fixed to $b_s = 6mm$ and $b_r = 2.0$ using a biweighted kernel for $K(x)$.

Region Fusion Depending on the data and the MeS parameters, the number of regions can be very high. In homogeneous regions the density gradient is near zero which may cause oversegmentation. For this reason, to reduce the number of meaningless regions two steps are normally applied to the MeS results: region merging and pruning.

Our region fusion method merges the spatially neighboring regions, r_i, r_j, when the intensity distance, $dist(M^{r_i}, M^{r_j})$, between their modes, M^{r_i}, M^{r_j} is less than a threshold t. Our implementation avoids the creation of a Region Adjacency Graph [9], using a union-find algorithm with the regions to be merged. All regions are merged at the same time instead of by pairs [6], in order to avoid a staircase effect. The final mode of the fusion region is the mean of the modes weighted by the size of the region associated to each mode.

Small regions follow a pruning process. Regions r_i, whose size is smaller than a size $s = S$, are automatically merged with the neighboring region with minimum $dist(M^{r_i}, M^{r_j})$. Small regions can only be merged with regions larger than s, so the pruning process is done iteratively from $s = 2, ..., S$. This pruning process stops with $S = 3$ because the minimal size of MS white matter lesions is defined as 3mm^3 [13].

Region Classification & Outliers Detection (Classification) We compute the Mahalanobis distance between the mode of each region in the image and each NABT given the previously computed parameters. Considering that voxels intensities in each NABT follows a Gaussian law, these Mahalanobis distances follow a χ^2 law with m degrees of freedom [2, 5]. Each region in the image is defined as an outlier if the Mahalanobis distance for every class is greater than the threshold defined by the χ^2 law, for a given p-value. Regions that are not considered as outliers are then classified in the class yielding their lowest Mahalanobis distance [10].

MS Rules White matter lesions are hyperintense compared to the WM in T2-w, Proton Density (PD-w) and FLAIR sequences [13], these intensity characteristics differentiate them from other outliers, e.g. noise, skull-stripping errors or vessels. For this reason, expert knowledge is formalized and applied in order to correctly classify the WML [2]. First, MS white matter lesions have to be hyperintense, so $I_{seq}(M_{ri}) > \mu_{seq}^{WM} + t_{seq}^{rules} * \sigma_{seq}^{WM}$ for $seq = T2, PD, FLAIR$,

where $I_{seq}(M^{ri})$ is the value of the mode for the sequence *seq*, and μ_{seq}^{WM} and σ_{seq}^{WM} are the mean and standard deviation of the white matter for the same sequence. t_{seq}^{rules} is a parameter chosen equal to 3 in our experiments. As we focus in WM lesions, all detections that are not contiguous to the WM are removed.

3 Validation & Results

3.1 Validation

The proposed algorithm is compared to three other similar algorithms in order to assess its performance:

- A: the proposed algorithm.
- B: as algorithm A but using the classical EM algorithm, similar to Mayer et al. [10].
- C: instead of classifying the MeS regions, each voxel is classified independently with the mEM algorithm, similar to Ait-Ali et al. [2].
- D: as algorithm C but using the classical EM algorithm instead of the mEM.

We evaluate the impact of using mEM instead of EM (A vs. B and C vs. D) and using the MeS algorithm compared to a standard global likelihood-based, approach (A and B vs. C and D).

Synthetic images We used the three sequences (T1-w, T2-w and PD-w) of the simulated MS brain from Brainweb [14], used with 3% of noise (n) and 0%, 20% and 40% of inhomogeneity (rf) and moderate lesion load. For these datasets the ground truth is known. For validation, we compared the ground truth with the automatic segmentation, the Dice Similarity Coefficient (DSC) [15] is used for MS white matter lesions.

Real images Images from seven different MS patients were acquired on a Philips 1.5T Gyroscan: 3-mm axial slice thickness T1-w, T2-w and PD-w. Images were denoised, corrected for intensity inhomogeneity, normalized in the stereotaxic space [16] and skull-stripping was performed [17]. WML were manually segmented by an expert and validation was done using the DSC.

3.2 Results

Results on BrainWeb phantom Table 1 shows that MeS improves WML segmentation for all levels of inhomogeneity and EM algorithm outperforms mEM for all levels of inhomogeneity. The reason for these results is that the phantom does not contain as much outliers as real images, in such cases mEM is removing too many NABT voxels from the estimation making a less precise estimation. In spite of this imprecise estimation, algorithm A manages to perform a good segmentation, showing the robustness of this method.

If we compare our results with other methods already published, we can observe that the DSC of our algorithm (0.87) for Brainweb with 3% of noise and no inhomogeneity is better than Rousseau's [18] (0.63) ,Freifeld's [19] (0.77) or Van-Leemput's [4] (0.80, calculated in[19]).

Results on real images In the real images, the EM algorithm fails to estimate the NABT model in all patients (algorithms B and D), which shows the limitation of the phantom studies. One example of false tissue classification can be seen in Figure 2. In these images tissue contrast is weak and there are multiple skull-stripping errors, making the EM unstable. The algorithm A slightly improves the results of algorithm B and also shows less variance in its results as shows Table 1, the robustness of algorithm A is that MeS regions are done with local information so their classification should be easier even if the model is not well estimated.

	BW n3rf0	BW n3rf20	BW n3rf40	Average Real	3D data
D	0,79	0.80	0.78	-	0.49
C	0,72	0.77	0.41	0.52 ± 0.07	0.66
B	**0,87**	0.84	**0.79**	-	0.43
A	**0,87**	**0.85**	0.63	**0.55 ± 0.05**	**0.67**

Table 1. DSC values for WML for the different images.

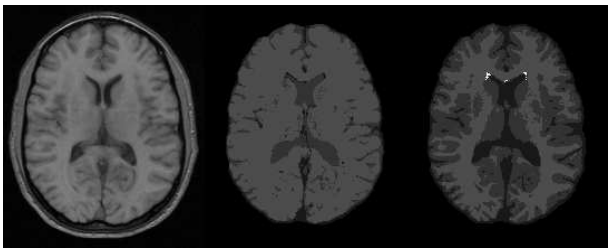

Fig. 2. Example of classification error of the EM algorithm. From left to right: T1-w, algorithm D results, algorithm C results.

4 Discussion & Conclusion

A new algorithm for WML and NABT segmentation has been presented that combines global and local information. This fusion of global and local information shows better results than only using global information. The idea of using a totally local method, as MeS, for MS segmentation is an innovation to our knowledge. We have also shown that the use of a robust estimation of parameters with mEM is crucial in order to correctly segment real images with this method [10].

Other MR acquisition protocols for MS include inversion recovery MR sequences, mainly FLAIR, because of their higher sensitivity for WML detection.

We have tried our algorithm with MS patients images from a 3T Siemens TRIO (1mm isotropic 3D T1-w, 1mm isotropic 3D T2-w and 1mm isotropic 3D FLAIR) yielding satisfying results for the proposed method. DSC results are displayed in Table 1 and in Figure 3. The use of 1mm isotropic images improves the spatial information by improving the results compared to the images used in the validation. In addition, the use of FLAIR sequence instead of PD further improved the results as the tissue contrast and lesion conspicuity is better in the former MR sequences. A direct comparison was not yet performed as we had no PD images with this resolution.

This method is an interesting novel idea for MS brain segmentation but requires further improvements. For example, the inclusion of bias field estimation or the automatic estimation for the parameters of the mean shift.

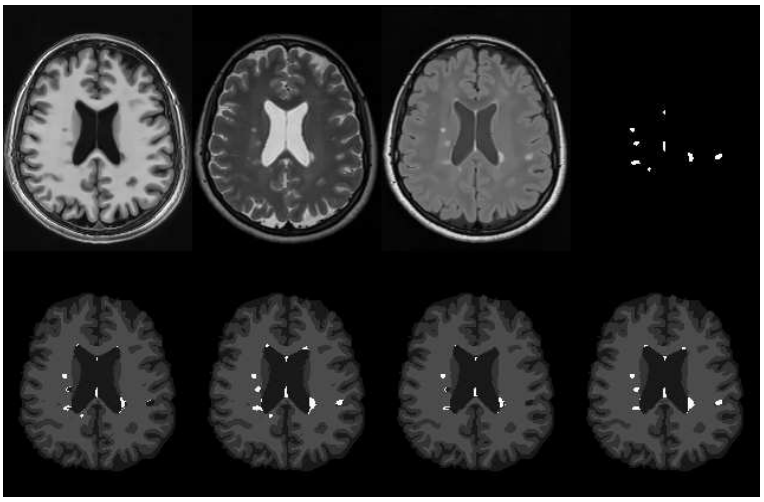

Fig. 3. Fully 3D protocol. Top, from left to right: T1-w, T2-w and FLAIR and WML manual segmentation. Bottom, from left to right: algorithms D, C, B and A.

References

1. Miller, D.H., Grossman, R.I., Reingold, S.C., McFarland, H.F.: The role of magnetic resonance techniques in understanding and managing multiple sclerosis. Brain **121 (Pt 1)** (Jan 1998) 3–24
2. Aït-Ali, L.S., Prima, S., Hellier, P., Carsin, B., Edan, G., Barillot, C.: STREM: a robust multidimensional parametric method to segment MS lesions in MRI. Med Image Comput Comput Assist Interv Int Conf Med Image Comput Comput Assist Interv **8**(Pt 1) (2005) 409–416

3. Atkins, M.S., Drew, M.S., Tauber, Z.: Towards automatic segmentation of MS lesions in PD/T2 MR images. In Hanson, K.M., ed.: Proc. SPIE Vol. 3979, p. 800-809, Medical Imaging 2000: Image Processing, Kenneth M. Hanson; Ed. Volume 3979 of Presented at the Society of Photo-Optical Instrumentation Engineers (SPIE) Conference. (June 2000) 800–809
4. Van Leemput, K., Maes, F., Vandermeulen, D., Colchester, A., Suetens, P.: Automated segmentation of multiple sclerosis lesions by model outlier detection. Medical Imaging, IEEE Transactions on **20**(8) (Aug. 2001) 677–688
5. Dugas-Phocion, G., Gonzalez, M., Lebrun, C., Chanalet, S., Bensa, C., Malandain, G., Ayache, N.: Hierarchical segmentation of multiple sclerosis lesions in multisequence MRI. In: Biomedical Imaging: Macro to Nano, 2004. IEEE International Symposium on. Volume 1. (April 2004) 157–160
6. Haris, K., Efstratiadis, S., Maglaveras, N., Katsaggelos, A.: Hybrid image segmentation using watersheds and fast region merging. Image Processing, IEEE Transactions on **7**(12) (Dec 1998) 1684–1699
7. Fukunaga, K., Hostetler, L.: The estimation of the gradient of a density function, with applications in pattern recognition. Information Theory, IEEE Transactions on **21**(1) (Jan 1975) 32–40
8. Comaniciu, D., Meer, P.: Mean shift: a robust approach toward feature space analysis. Pattern Analysis and Machine Intelligence, IEEE Transactions on **24**(5) (May 2002) 603–619
9. Jimenez-Alaniz, J., Medina-Banuelos, V., Yanez-Suarez, O.: Data-driven brain mri segmentation supported on edge confidence and a priori tissue information. Medical Imaging, IEEE Transactions on **25**(1) (Jan. 2006) 74–83
10. Mayer, A., Greenspan, H.: Segmentation of brain mri by adaptive mean shift. In: Biomedical Imaging: Macro to Nano, 2006. 3rd IEEE International Symposium on. (6-9 April 2006) 319–322
11. Dempster, A.P., Laird, N.M., Rubin, D.B.: Maximum Likelihood from Incomplete Data via the EM Algorithm. Journal of the Royal Statistical Society **39**(1) (1977) 1–38
12. Neykov, N., Filzmoser, P., Dimova, R., Neytchev, P.: Robust fitting of mixtures using the trimmed likelihood estimator. Computational Statistics & Data Analysis **52**(1) (September 2007) 299–308
13. Barkhof, F., Filippi, M., Miller, D.H., Scheltens, P., Campi, A., Polman, C.H., Comi, G., Adèr, H.J., Losseff, N., Valk, J.: Comparison of MRI criteria at first presentation to predict conversion to clinically definite multiple sclerosis. Brain **120 (Pt 11)** (Nov 1997) 2059–2069
14. Collins, D., Zijdenbos, A., Kollokian, V., Sled, J., Kabani, N., Holmes, C., Evans, A.: Design and construction of a realistic digital brain phantom. Medical Imaging, IEEE Transactions on **17**(3) (Jun 1998) 463–468
15. Zijdenbos, A., Dawant, B., Margolin, R., Palmer, A.: Morphometric analysis of white matter lesions in mr images: method and validation. Medical Imaging, IEEE Transactions on **13**(4) (Dec 1994) 716–724
16. Zijdenbos, A.P., Forghani, R., Evans, A.C.: Automatic "pipeline" analysis of 3-D MRI data for clinical trials: application to multiple sclerosis. IEEE Trans Med Imaging **21**(10) (Oct 2002) 1280–1291
17. Smith, S.M.: Fast robust automated brain extraction. Hum Brain Mapp **17**(3) (November 2002) 143–155
18. Rousseau, F., Blanc, F., de Seze, J., Rumbach, L., Armspach, J.P.: An a contrario approach for outliers segmentation: Application to Multiple Sclerosis in MRI. In:

Biomedical Imaging: From Nano to Macro, 2008. ISBI 2008. 5th IEEE International Symposium on. (14-17 May 2008) 9–12
19. Freifeld, O., Greenspan, H., Goldberger, J.: Lesion Detection in Noisy MR Brain Images Using Constrained GMM and Active Contours. In: Biomedical Imaging: From Nano to Macro, 2007. ISBI 2007. 4th IEEE International Symposium on. (12-15 April 2007) 596–599